Journal of the European Ceramic Society 21 (2001) 1919–1923

www.elsevier.com/locate/jeurceramsoc

Effect of nano-particles SnO_2 and CeO_2 addition on the Y123/Y211 sample grown in a microwave furnace

S. Marinel *, G. Desgardin

Laboratoire CRISMAT, UMR CNRS-ISMRa 6508, 6 Bd Maréchal Juin, 14050 Caen cedex, France

Received 4 September 2000; received in revised form 14 November 2000; accepted 18 December 2000

Abstract

It is well known that the critical current density (J_c) of Y123 bulk superconductor can be increased by the introduction of non superconducting flux pinning centers such as small secondary phases precipitates (1 μm^3). Thus, several studies have shown that the introduction of CeO_2 and SnO_2 powders allows the formation of micron size secondary phases homogeneously distributed in the Y123 matrix allowing an increasing of J_c. As the precipitates size should be a crucial parameter that affects pinning properties of Y123, this work is devoted to compare, in terms of microstructure and superconducting properties, the effect of micrometric and nanometric SnO_2 particles addition in the '$SnO_2 + CeO_2$' doped sample. It was shown that the addition of nanometric SnO_2 particles, compared with an addition of micronic SnO_2 particles, induces an increasing of the reactivity between the liquid phase and the dopants. Then, Y211 coarsening is not reduced and micronic secondary phases is formed conducting to obtain no improvement of the superconducting properties.

Keywords: Microwave processing; Oxide superconductor

1. Introduction

The improvement of critical current density (J_c) of high-T_c superconductors is one of the most important problems to overcome in order to develop high current applications. Up to now, the melt textured growth process has been used to reduce the grain boundary density to allow significantly increased J_c.[1] It is also well known that the introduction into the Y123 matrix of small non-superconducting precipitates (with micronic size usually) can play the role of pinning centers allowing thus an improvement in J_c.[2] Even if the reasons behind this increase are numerous and not yet perfectly defined, the introduction of such non superconducting precipitates is undoubtedly interesting from a technological point of view. For this goal, doping with SnO_2[2] or CeO_2[3] was widely studied and more recently, we also demonstrated how the combination of these two oxides can be beneficial in improving both J_c and Y123 growth rates using two distinctive processes, i.e. the microwave melt process[4] and the classical top-seeding-melt texture growth process (TSMTG).[5] Furthermore, He et al. have tested the introduction of SnO_2 nano-particles in the CeO_2 doped Y123 using the TSMTG process in order to obtain finer precipitates and thus J_c improvement.[6] However, they found that even with such doped elements, no J_c improvement was observed. Furthermore, the J_c vanishing was found to be more significant as the Sn content increases. These first results are interpreted as the consequence of the drag force law determined by Uhlmann et al.[7] Indeed, the drag force (f) is given by the following equation:

$$f = 6\pi\eta R_0^2 \frac{v}{d_s}$$

where η is the melt viscosity, R_0 the mean particle radius, v the growth front velocity and d_s the distance between particle and the growth front. Thus, since the melt viscosity decreases as the SnO_2 content increases[4] the viscous drag force is also reduced, which is favorable to the pushing particle phenomenon. Moreover, the drag force is as low as the particle size is low. Consequently, these two phenomena are consistent with the

* Corresponding author. Tel.: +33-02-31-45-29-15; fax: +33-02-31-95-416-00.

E-mail address: marinel@ismra.fr (S. Marinel).

0955-2219/01/$ - see front matter
PII: S0955-2219(01)00143-1

fact that the introduction of SnO_2 nano-particles implies that the trapping of both small Y211 precipitates and obviously small precipitates (nanometric size) is not encouraged. This interpretation may explain why no such improvement in J_c was observed. However, the drag force law shows also that this factor is proportional to the growth front velocity. The higher the growth front velocity, the higher the viscous drag force obtained. This work investigates the possibility of trapping finer particles using the microwave melt process method which allows to obtain single-domain Y123 to be obtained at higher speed than other processes.[4]

2. Results and discussion

The microwave device described in a previous paper[8] applies a maximum temperature of 1070°C with a thermal gradient close to 200°C/cm at about 980°C, i. e. at a temperature approximately equal to the Y123 peritectic temperature. The study was performed using commercial grade 123 powder (Solvay 99.9%), CeO_2 (Aldrich, 99.9%), SnO_2 (Prolabo, 99%) and SnO_2 nano-particles prepared by He et al. using a sol–gel method.[9] The average particle size of nano-particles was about 20 nm (see Ref. 6) and, for the commercial SnO_2, the mean particle size was about 3 μm. Y_2BaCuO_5 (Y211, mean particle size 0.6 μm) was prepared by a solid state reaction using stoichiometric rations Y_2O_3 (Neyco, 99.99%), $BaCO_3$ (Prolabo, 99.5%) and CuO (Prolabo, 99%) which were subsequently milled to form an intimate mixture using ZrO_2 balls in absolute ethanol. Different mixtures of Y123/Y211 (1 / 0.3 mol ratio) doped with 0.5 wt.% of CeO_2 and with different amounts of SnO_2 were prepared by thoroughly mixing in an agate ball mill for 45 min. Table 1 depicts the different compositions prepared with their respective name versus the SnO_2 origin. These precursors were then prepared into bar-shaped pellets by isostatically pressing of the powdered mixture at 300 MPa using a latex tube as a dye (15–20 cm length, 1.2 cm inner diameter). Each bar was then fixed on the jaw drill and was translated through the microwave cavity at 2 mm/h from the bottom to the top. Samples obtained were then longitudinally polished and characterized using scanning electron microscopy coupled with an EDS analysis system (Phillips XL'30 and Link Isis Oxford system respectively). To determine the superconducting properties, small cleaved samples were extracted from each bar and were annealed under oxygen flow. A squid magnetometer was used to measure the critical temperature and the inductive critical current density using the modified Bean model.[10] Regardless of the SnO_2 particle size and amount, samples were found to be mainly single-domain as obtained previously.[8] In terms of microstructure, the main difference was the Y211 size in the matrix after the melt texturing process. Indeed, the Y211 size, for the same SnO_2 level is bigger in the case of an addition of SnO_2 nano-particle than in the micro-particle case. To demonstrate this behavior without any ambiguity, 2 pellets prepared with the composition m3 and n3 were heated at 1070°C for 72 h and then quenched at room temperature. The obtained pellets were then treated with a bromo-ethanol solution for dissolving the solidified liquid phase and SEM observations were performed in order to observe the Y211 size and morphology (see Fig. 1). For an addition of nano-particle, the Y211 maximum size is close to 15–16 μm (case-B-) compared with the other precipitates which are smaller than 8–9 μm (case-A-) confirming observations performed on the Y123 matrix. Moreover, in the case of an addition of SnO_2 nano-particles, the

Table 1
This describes the SnO_2 amount and granulometry with the name for each sample. The molar percentage of SnO_2 is based on Y123 mol

Molar% of SnO_2	SnO_2 micronic size	SnO_2 nanometric size
0.1	M1	N1
0.3	M2	N2
0.5	M3	N3
0.7	M4	N4

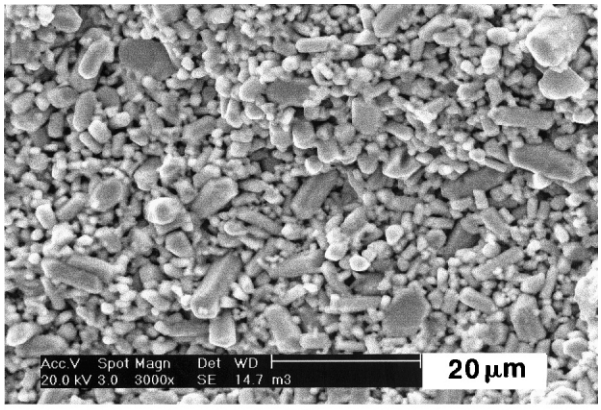

Fig. 1. Y211 coarsening versus the initial SnO_2 size (a) micro-particle and (b) nano-particle.

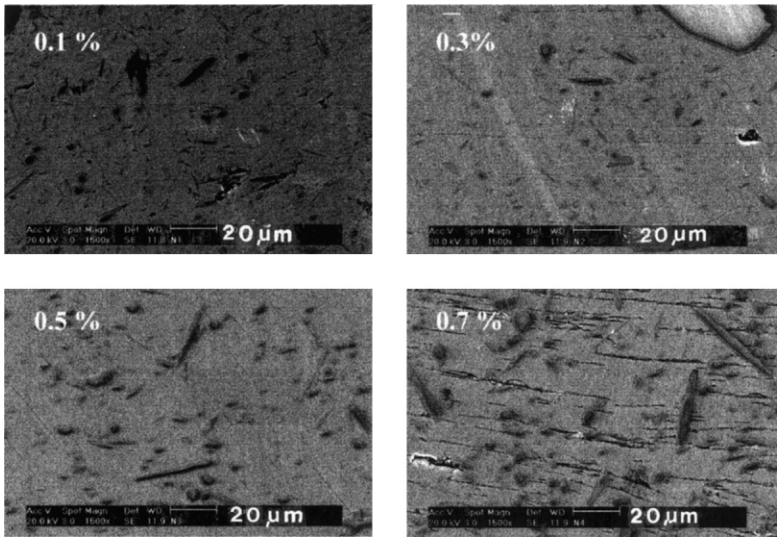

Fig. 2. Y211 particle size versus the initial SnO_2 content.

Y211 coarsening increases as the tin doping increases (Fig. 2). The precipitate coarsening in the liquid phase is governed by the following equation:[4]

$$R_{Y211} \propto \left(\frac{\sigma}{\eta}\right)^{1/3}$$

where σ is the interfacial energy between the Y211 surface and the liquid phase. Accordingly the observation, the introduction of SnO_2 nano-particles is observe to increase the effect of SnO_2 in terms of viscosity. Indeed, we know that SnO_2 addition decreases the melt viscosity and then increases the precipitates coarsening but when micro-particles are used, this effect is very slight.[4] In the case of an addition of SnO_2 nano-particles, the coarsening of Y211 versus an increasing of the SnO_2 content is obvious confirming the effect of the SnO_2 size on the liquid viscosity. Our conviction is that the reactivity is exacerbated when nano-particles are used compared with an addition of SnO_2 micro-particles. This result in terms of microstructure seems to be the major difference between samples doped with SnO_2 nano-particles or micro-particles. Indeed, the distribution and size of secondary phases are quite similar and independent of the SnO_2 size, i.e. a non-perfect uniform distribution with the presence of precipitates which are agglomerated (Fig. 3). Moreover, the phase composition seems to be similar to

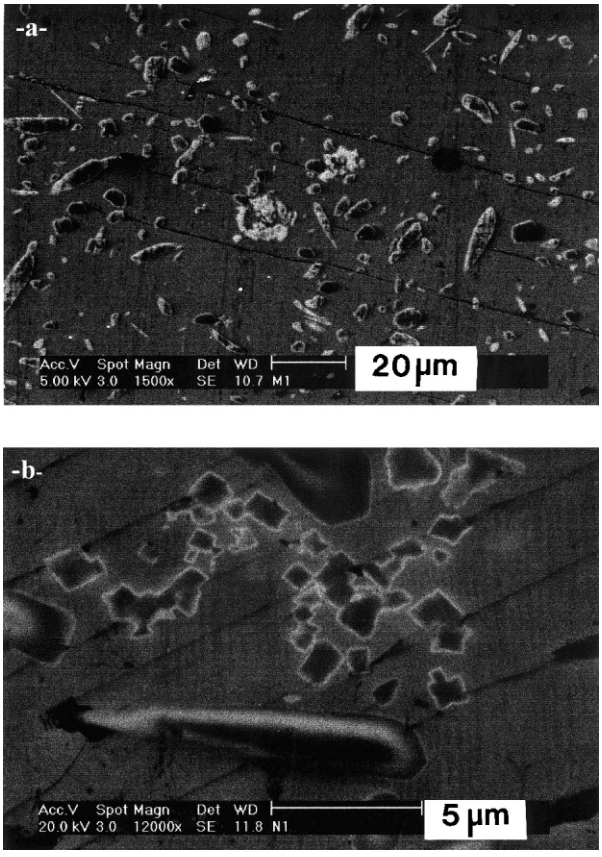

Fig. 3. Secondary phase morphologies and distribution versus initial SnO_2 size (a) micro-particle and (b) nano-particle.

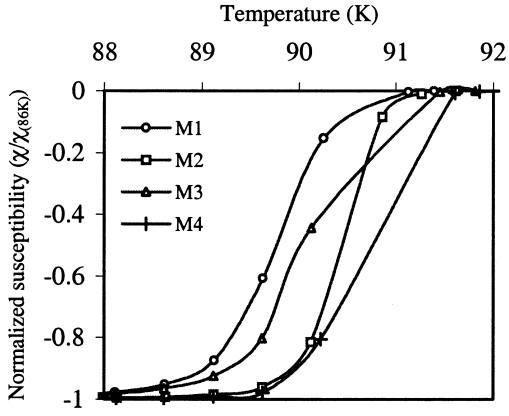

Fig. 4. Critical temperature of sample doped with SnO_2 micro-particle versus the tin doping level.

the Φ_2 phase observed previously,[4] i.e. a Ba–Y–Cu–Sn–Ce–O phase from both cases according to EDS analysis. To conclude the microstructural observations, the addition of SnO_2 nano-particles exacerbates the effect of such addition, i. e. the viscosity decreases and the reactivity increases. The Y211 precipitates coarsening is not limited. As a result, larger Y211 precipitates develop in the matrix compared to those formed with the addition of SnO_2 micro-particles.

Furthermore, due to the high reactivity between SnO_2 and the liquid phase, no major difference is observed in terms of precipitate size and distribution.

Concerning the superconducting properties, the critical temperature obtained from the magnetization measurements is given in Fig. 4. The T_c onset increases with the tin doping level as we have previously observed.[4] This confirms that tin doping allows the impurities to drain away from the matrix. Moreover, the T_c range is very sharp and even if this tendency can be observed, the T_c onset varies fluently from 91.1 to 91.7 K, respectively for M1 and for M4 while the ΔT_c are nearly the same for all samples (close to 2 K). Samples doped using SnO_2 nano-particles exhibit approximately the same T_c and ΔT_c curves but the dependence with the tin doping level is more erratic showing less homogeneous sample microstructure. The J_c without applied magnetic field is very high in both cases with a record for the sample N4 at 65000 A/cm^2 (see Fig. 5). However, the main difference versus the initial SnO_2 size is the J_c under field ($H > 1$ Tesla). When nano-particles are used, the J_c under high field decreases drastically compared with the other samples. Thus, the imperfect uniformity of the secondary phase precipitate distribution combined with bigger Y211 particles in the matrix is probably responsible for the low J_c in high field.

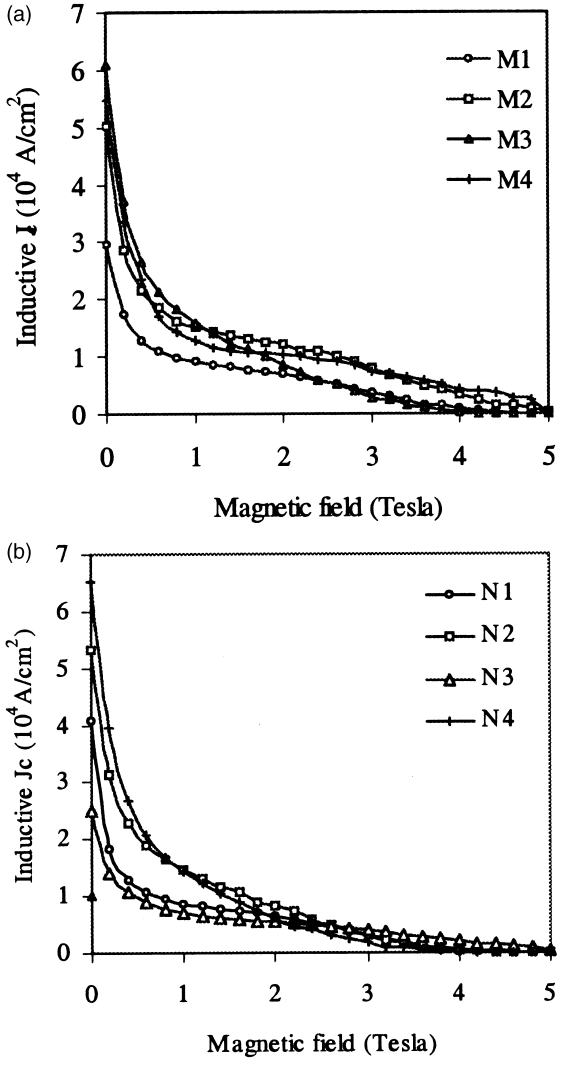

Fig. 5. Inductive J_c obtained from the magnetization loop at 77 K for samples doped using (a) SnO_2 micro-particles and (b) nano-particles .

3. Conclusion

No beneficial effect of SnO_2 nano-particles addition was found in comparison with micronic size SnO_2 powder. To realize beneficial effects in the microwave melt process, (i.e. to process Y123 textured material at relatively high speed), it should be envisaged to add nano-particles of doping element having less affinity with the liquid phase.

Acknowledgements

The authors thank Dr. Zhenhui He from the University of Zhongshan for graciously preparing the SnO_2 nano-particles powder.

References

1. Salama, K., Selvamanickam, V., Gao, L. and Soon, K., High current density in bulk $YBa_2Cu_3O_{7-\delta}$ superconductor. *Appl. Phys. Lett.*, 1989, **52**, 2352–2354.
2. Osamura, K., Matsukura, N., Kusumoto, Y., Ochiai, S., Ni, B. and Matsushita, T., Improvement of critical current density in $YBa_2Cu_3O_{7-\delta}$ superconductor by Sn addition. *Jpn. J. Appl. Phys.*, 1990, **29**, L1621–L1623.
3. Sandiumenge, F., Pinol, S., Obradors, X., Snoeck, E. and Rouceau, C., Microstructure of directionally solidified high-critical-current $YBa_2Cu_3O_{7-\delta}$–Y_2BaCuO_5 composites. *Phys. Rev. B*, 1994, **50**, 7032–7044.
4. Marinel, S., Monot, I., Provost, J. and Desgardin, G., Effect of SnO_2 and CeO_2 doping on the microstructure and superconducting properties of melt textured zone $YBa_2Cu_3O_{7-\delta}$. *Supercond. Sci. Technol.*, 1998, **11**, 563–572.
5. Leblond-Harnois, C., Marinel, S., Monot-Laffez, I., Bourgault, D., Desgardin, G. and Raveau, B., High critical curent in Ce/Sn doped YBCO pellets grown by top seeding method. In *Applied. Superconductivity*, Vol. 1. IOP publishing series number 167, 1999, pp. 63–66.
6. He, Z. H., Surzhenko, O. B., Habisreuther, T., Zeisberger, M. and

Gawalek, W., Preliminary investigation on the superconducting properties of textured $YBa_2Cu_3O_{7-\delta}/Y_2BaCuO_5$ grown with the addition of nanoparticles. In *Applied Superconductivity*, Vol. 1, IOP publishing series number 167, 1999, p. 151.
7. Uhlmann, D. R., Chalmers, B. and Jackson, K. A., Interaction between particles and a solid–liquid interface. *J. Appl. Phys.*, 1964, **35**(10), 2986–2993.
8. Marinel, S., Bourgault, D., Belmont, O., Sotelo, A. and Desgardin, G., Microstructure and transport properties of YBCO zone melted samples processed in a microwave cavity and infra-red furnace. *Physica C*, 1999, **315**, 205–214.
9. He, Z. H., Wu, M. Z., Bruchlos, G., Xiong, X. M., Luo, Y. Y. and Gawalek, W., $Y_2Ba_5(_{Sn3-y-z}Cu_yPt_z)O_x$ in textured YBCO superconductors. *Physica C*, 1999, **312**, 261–268.
10. Bean, C. P., Magnetization of high-field superconductors. *Review of Modern Physics*, 1964, **36**, 31–39.